SUSCEPTIBILITY TENSOR IMAGING OF THE RENAL TUBULE

Luke Xie[1,2], Russell Dibb[1,2], Wei Li[3], Chunlei Liu[2,3], and G. Allan Johnson[1,2]

[1]Department of Biomedical Engineering, Duke University, Durham, North Carolina, United States, [2]Center for In Vivo Microscopy, Duke University Medical Center, Durham, North Carolina, United States, [3]Brain Imaging Analysis Center, Duke University Medical Center, Durham, North Carolina, United States

Purpose

Major functions of the renal system depend on the complex 3D structure and organization of the uriniferous tubule. It has been suggested that the integrity and architecture of the tubules may be assessed with diffusion tensor imaging (DTI) (1). However, we found that DTI was only able to track tubules in the inner medulla of the kidney. It failed to find any coherent tracts in the outer medulla. The purpose of the study was to determine whether susceptibility tensor imaging (STI) was able to overcome this limitation. We report that STI was able to track tubules in the whole kidney including the inner medulla (IM), outer medulla (OM), and cortex (CO). STI may offer a powerful method to study renal structure and function that overcomes limitations of current techniques.

Methods

Perfusion & fixation: Studies were performed on a kidney from a C57Bl/6 mouse. The kidney was perfusion fixed (10% formalin) and scanned for STI. Subsequently, the kidney was immersion enhanced with ProHance (2.5mM). ProHance is a Gd contrast agent used to actively stain and decrease T1 relaxivity (2). After immersion, STI scan was repeated and DTI scan was conducted. The kidney was then processed and prepared for microscopy to validate MRI results.

MRI: MRI was performed in a vertical bore 9.4T Oxford magnet. The specimen was placed in a spherical holder to facilitate multiple orientations for STI. The holder was placed in a high Q loop gap resonator. STI data were acquired using 3D multi-echo gradient echo sequence. After phase processing and correction, individual echo datasets were summed to increase the SNR (3). The SNR gains achieved were: ~ 3x for non-contrast enhanced kidney (16 echoes) and ~ 2x for contrast enhanced kidney (6 echoes). DTI data were acquired using a 3D diffusion-weighted spin echo sequence. One b_0 image and six images with diffusion weighting (1500 s/mm^2) were acquired. Images were acquired at 54.7μm^3.

STI and tractography: Image phase at 17 orientations were used to solve for the 6 independent elements of the susceptibility tensor (χ_{11}, χ_{12}, χ_{13}, χ_{22}, χ_{23}, and χ_{33}) following (4). Eigenvalue decomposition was performed on the tensor to define the 3 principal susceptibilities and eigenvectors. Tractography was performed on major diamagnetic eigenvector, seeded by mask images, and filtered by renal regions and track lengths (TrackVis). Angle threshold was 60°. DTI FA threshold was 0.1 to 0.9.

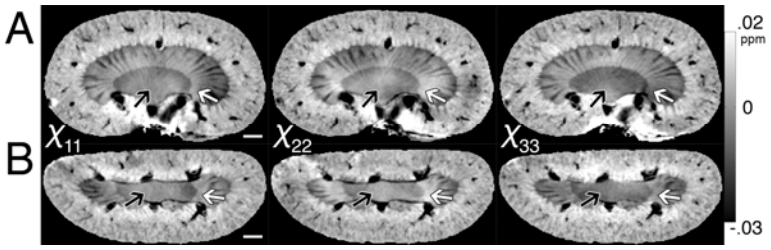

Fig 1. Diagonal elements of the susceptibility tensor array in coronal view (A) and sagittal view (B). Black arrow points to IM and white arrow points to OM. Images were inverted to emphasize renal parenchyma. Scalebars=1mm.

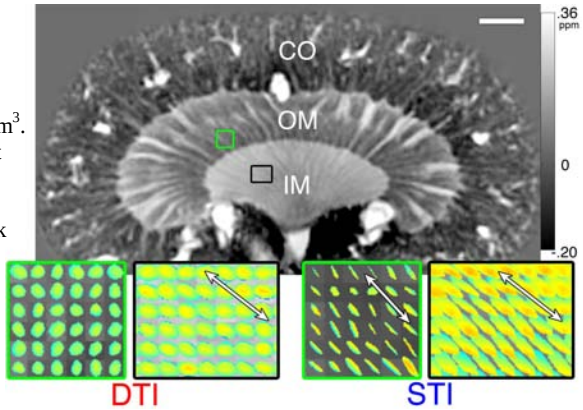

Fig 2. Susceptibility tensor summed image. Green box shows an OM region. Black box shows an IM region. DTI and STI tensor glyphs shown for these IM and OM regions. White arrows point to overall direction of eigenvectors.

Results

Fig. 1 shows the diagonal elements of susceptibility tensor array. The alternation of contrast across the tensor elements is noticeable in the renal regions, which indicate anisotropic susceptibility. Fig. 2 shows the tensor glyphs from DTI and STI in an IM and OM region. DTI shows no anisotropy in the OM, while STI shows strong anisotropy. Fig. 3 shows the tractography of DTI (Fig. 3A) and STI (Fig. 3B-D). Tracks point out of the IM to the tip of the papilla (Fig. 3C). Additional tubules were tracked in the most medial part of the CO (Fig. 3D). In DTI and STI, IM tracks fanned out in anteroposterior direction and mediolateral direction.

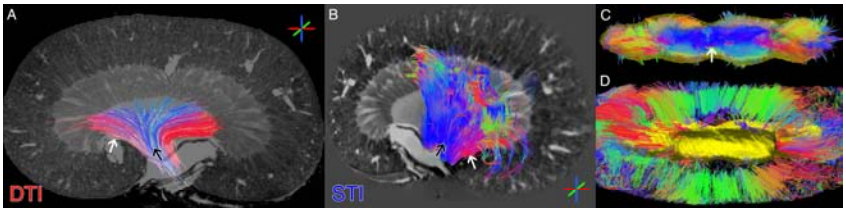

Fig 3. A: DTI tracks overlaid on transparent b_0 image. B: STI tracks overlaid on transparent susceptibility image. Arrows point to corresponding areas in DTI tracks. STI tracks extend from IM to OM. C: IM/OM tracks shown with OM surface render. D: Tracks in the most medial part of CO. OM surface render shown without IM/OM tracks. Color axis: red=anteroposterior, green=dorsoventral, and blue=mediolateral.

Discussion and Conclusion

The length and tortuosity of the murine nephron beyond the cortex are essential for the kidney to achieve extraordinary concentrations of urine (5). Studying these structures non-destructively is challenging. While DTI provides excellent reconstruction of tubules in the IM, it fails to reconstruct meaningful tracts in the OM and CO even with a generous FA threshold. No coherent DTI eigenvectors were found beyond the region of IM. Surprisingly, STI exhibits strong anisotropy in the OM. STI tractography was able to reconstruct tubules in all three regions. To understand the underlying mechanism, we acquired confocal microscopy of the kidney. In the IM, the tubules were straight and coherent. The OM contained mostly tortuous tubules. This tortuosity resulted in incoherent diffusion eigenvectors. The medulla thick ascending limbs in the OM, though straight, have larger diameters and reduced diffusion anisotropy compared to tubules in the IM. STI anisotropy, on the other hand, is determined by the molecular composition and ordered cellular arrangement of the tubules. Similar to the model of lipids creating anisotropy in neuroimaging (6), the anisotropy observed here is likely due to the lipid organization in renal epithelia. We found that the major STI eigenvector pointing in the tubule axis was associated with the largest diamagnetic susceptibility. The lipids of renal epithelia, which are very diamagnetic, also point along the tubule axis. In summary, STI was able to detect straight tubules across the entire kidney, while DTI was limited to one renal region. STI provides a novel contrast mechanism for the kidney where contrast can be directly related to local tubule microstructure and molecular composition.

References

[1] Gaudiano C et al. *MRI* 29: 1030-33, 2011. **[2]** Johnson GA et al. *JMRI* 16: 423-29, 2002. **[3]** Wu B et al. *NeuroImage* 59: 297-305, 2012. **[4]** Liu C. *MRM* 63: 1471-77, 2010. **[5]** Zhai XYet al. *JASN* 17: 77-88, 2006. **[6]** Li W et al. *NeuroImage* 59: 2088-97, 2012.